PCCP

Electron paramagnetic resonance and diffuse reflectance spectroscopic studies of the photoionization of *N*-alkylphenothiazines in synthetic microporous M-clinoptilolite (M = $Na^+ + K^+$, H^+, Li^+, Na^+, K^+, Ni^{2+}, Co^{2+}, Cu^{2+}) molecular sieves at room temperature

R. M. Krishna, Zhixiang Chang, Hosun Choo, Koodali T. Ranjit and Larry Kevan*

Department of Chemistry, University of Houston, Houston, TX 77204-5641, USA

Received 10th April 2000, Accepted 24th May 2000
Published on the Web 29th June 2000

Methylphenothiazine and other *N*-alkylphenothiazines were incorporated into M-clinoptilolite (M = $Na^+ + K^+$, H^+, Li^+, Na^+, K^+, Ni^{2+}, Co^{2+}, Cu^{2+}) channels by impregnation. Photoionization of *N*-alkylphenothiazines (PC_n) doped into dehydrated M-clinoptilolite samples at room temperature by ultraviolet irradiation results in the formation of *N*-alkylphenothiazine radical cations ($PC_n^{\cdot+}$). The radicals were identified by the electron paramagnetic resonance (EPR) *g*-factor and by diffuse reflectance spectroscopy. Dehydrated M-clinoptilolites are efficient hosts for the formation and stabilization of PC_n^+ at room temperature. As-synthesized M-clinoptilolite that was not dehydrated and then doped with PC_n was EPR silent. The PC_n^+ yield was determined by double integration of the EPR spectrum. The PC_n^+ yield is highest in H-clinoptilolite among the other ion-exchanged M-clinoptilolites. The photoionization efficiency to form PC_n^+ decreases in the order H-clinoptilolite > Ni-clinoptilolite > K-clinoptilolite > Na-clinoptilolite > Co-clinoptilolite > Na,K-clinoptilolite > Li-clinoptilolite > Cu-clinoptilolite. The photooxidation yields decrease as the PC_n alkyl chain length increases from methylphenothiazine (PC_1) to decylphenothiazine (PC_{10}). The photoionization efficiency depends on the nature of the metal ion and the channel size of the M-clinoptilolite material.

Introduction

Substantial effort is being directed toward the development of stable and efficient photosynthetic systems for the conversion and storage of solar energy into chemical energy.[1–6] In these photochemical processes, chemical energy is stored in a charge separated state (D^+A^-). In artificial systems a major goal is to produce net charge separation, since efficient photoionization followed by rapid ion recombination is not a route to practical energy storage. In homogeneous solution back-electron transfer and recombination of the photoproducts is typically fast. These processes can be slowed down in heterogeneous systems where the molecular mobility is restricted and the electron donors and one or more electron acceptors are spatially organized. Several significant results have been obtained in studies of model heterogeneous systems of vesicles,[7,8] micelles,[9,10] clays,[11,12] layered materials,[13–15] silica gels[16,17] and zeolites[18–20] containing photoactive molecules. The net photoyield of photoinduced charge separation has been increased and back-electron transfer has been slowed down significantly compared with homogeneous systems with similar photoactive molecules. Recent electron paramagnetic resonance (EPR) and diffuse reflectance studies of the photoionization and stabilization of photoproducts in microporous[21,22] and mesoporous[23] materials proved that efficient and long-lived charge separation can be achieved for hours or even several days at room temperature.

Recently, we have reported the photoinduced charge separation of *N*-alkylphenothiazines in microporous Na,K-ETS-10 and its ion-exchanged molecular sieves with different alkali metal ions, transition metal ions and protons.[21] These microporous crystalline materials show very efficient photoinduced electron transfer of PC_n and form a charge separated state which is long-lived and very stable in air for several days. Spectroscopic studies show that the photoproduct is a PC_n^+ radical cation, produced in Na,K-ETS-10 and its ion-exchanged materials. The stability of this charge separated state in Na,K-ETS-10 and its ion-exchanged materials increases with alkyl chain length due to an increased inductive effect in the PC_n^+ radical cations as a function of alkyl chain length.

Na,K-clinoptilolite is the most abundant natural zeolite and has found wide applications in ion-exchange, adsorption and catalysis.[24,25] Na,K-clinoptilolite molecular sieve is composed of 10-ring and 8-ring main channels parallel to each other along the *c*-axis. They are intersected by another 8-ring channel that runs along the *a*-axis. This leads to approximate channel dimensions of 7.2 × 4.4 Å. The negative charge of the Na,K-clinoptilolite framework from tetrahedrally coordinated aluminium is balanced by Na^+ and K^+ cations. The Na,K-clinoptilolite framework can be modified by varying the charge compensating cations *via* conventional ion-exchange to optimize electron transfer between photosensitive electron donors and acceptors.

In the present study, we have examined the photoionization of N-alkylphenothiazines loaded into Na,K-clinoptilolite (Na,K-Clino), H-clinoptilolite (H-Clino), Li-clinoptilolite (Li-Clino), Na-clinoptilolite (Na-Clino), K-clinoptilolite (K-Clino), Ni-clinoptilolite (Ni-Clino), Co-clinoptilolite (Co-Clino) and Cu-clinoptilolite (Co-Clino) molecular sieves and have found that the presence of protons, various alkali metal ions and transition metal ions in ion-exchanged sites of these Na,K-clinoptilolite/PC_n materials influences the photoyield of $PC_n^{\cdot+}$ radical cations. A combination of techniques, including X-ray diffraction (XRD), EPR, thermal gravimetric analysis (TGA) and UV–vis diffuse reflectance spectroscopy, were used to

monitor the photophysical properties of the M-clinoptilolite/PC_n (M = $Na^+ + K^+$, H^+, Li^+, Na^+, K^+, Ni^{2+}, Co^{2+}, Cu^{2+}; n = 1, 3, 6, 10) materials. The photoyield was found to depend on the nature of the metal ion and the channel size of the M-clinoptilolite. The photoyield and stability of the PC_n^{+} radical cation show the potential utility of microporous M-clinoptilolite molecular sieves for controlling the photoionization of PC_n (n = 1, 3, 6, 10) molecules.

Experimental section

Synthesis of Na,K-clinoptilolite

The synthetic Na,K-clinoptilolite molecular sieve was synthesized following the literature procedure.[26] Dried aluminium hydroxide, $Al(OH)_3$ (USP, Pfaltz & Bauer Inc.), 6 M NaOH solution, 6 M KOH solution, colloidal silica (Ludox LS, Aldrich) were used without further purification. Deionized water was used throughout the synthesis. Syntheses were carried out in 10 ml stainless steel autoclaves lined with Teflon™ at autogenous pressure without agitation. To decrease the crystallization time, seed crystals were added. In a typical Na,K-clinoptilolite synthesis, 0.87 g of dried aluminium hydroxide was added to a mixture of 0.54 ml 6 M NaOH and 2.46 ml 6M KOH solution. After stirring for about 1 h, 8.26 ml of colloidal silica was added slowly and the mixture was further stirred for 1 h. Finally, 0.1 g of seed crystals of synthetic Na,K-clinoptilolite was added to promote crystallization. The resulting gel was crystallized hydrothermally in Teflon™-lined autoclaves at 453 K for 4 days. The resulting gel pH of the mother liquor was 9.6. After crystallization the solid product was filtered off, washed with deionized water and dried in air at 343 K overnight. The molar composition of the final gel was $0.29NaOH : 1.33KOH : 1Al(OH)_3 : 4.5SiO_2 : 54.2H_2O$. The XRD pattern of this sample shows single phase, Na,K-clinoptilolite (Fig. 1).

Ion-exchange

To obtain H-clinoptilolite, synthetic Na,K-clinoptilolite was exchanged with 1 M ammonium chloride at 343 K overnight followed by washing. This procedure was repeated three times. The product was calcined in air at 673 K overnight to decompose the ammonium ion and obtain H-clinoptilolite.

To obtain M-clinoptilolite (M = Li^+, Na^+, K^+, Ni^{2+}, Co^{2+}, Cu^{2+}) samples were prepared *via* ion-exchange with the respective metal chloride stock solutions. A mixture of synthetic Na,K-clinoptilolite and the alkali metal or transition metal chloride 1 M stock solution was kept at 343 K while stirring overnight. This procedure was repeated three times to reach a maximum degree of ion-exchange. The final alkali metal or transition metal ion exchanged M-clinoptilolite was washed with distilled, deionized water several times and dried in air. The M-clinotilolite structure was retained after ion-exchange by metal ions and calcination based on the evidence of XRD patterns.

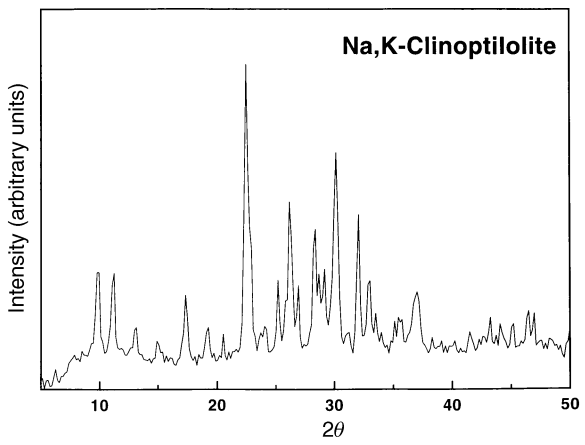

Fig. 1 X-Ray diffraction pattern of single phase crystalline Na,K-clinoptilolite.

Characterization

XRD powder patterns were recorded on a Siemens D 5000 X-ray diffractometer using Cu Kα radiation of wavelength 1.541 Å over the range $4° < 2\theta < 50°$. EPR spectra were recorded at room temperature at 9.5 GHz using a Bruker ESP 300 spectrometer with 100 kHz field modulation. The microwave power was maintained at 2 mW which is well below the saturation level for irradiated *N*-alkylphenothiazine samples. The microwave frequency was measured with a Hewlett Packard 5350 B frequency counter, and the magnetic field was monitored with a Bruker ER 032 M Hall effect field controller. The average value of the photoinduced $PC_1^{\cdot+}$ or $PC_n^{\cdot+}$ radical cation yield was determined from triplicate experiments for each system by double integration of the first derivative EPR spectra using the ESP 300 software. Diffuse reflectance UV–vis spectra were recorded before and after different times of photoirradiation at room temperature using a Perkin-Elmer model 330 spectrophotometer and a Hitachi integrating sphere. TGA of the samples was performed using a TGA 2050 analyzer from TA Instruments in an oxygen atmosphere at a heating rate of 10 °C min^{-1}.

Photoirradiation

All PC_n containing M-clinoptilolite (M = $Na^+ + K^+$, H^+, Li^+, Na^+, K^+, Ni^{2+}, Co^{2+}, Cu^{2+}) materials were photoirradiated using a 300 W Cermax xenon lamp (LX 300 UV) at room temperature. The power supply used was from ILC technology which was operated at 50% (10 A) of its rated maximum output power. For homogeneous irradiation of the samples, each sample was rotated at 4 rpm at room temperature. The irradiation passed through a filter combination consisting of 10 cm of water to absorb infrared radiation and a Corning glass filter, No. 7-54, to filter light of wavelengths shorter than 320 nm. The photoinduced $PC_n^{\cdot+}$ radical cations were identified by EPR and diffuse reflectance UV–vis spectroscopy.

Samples for photoionization

PC_n (n = 1, 3, 6, 10) was incorporated by immersing 0.5 g of each into M-clinoptilolite (M = $Na^+ + K^+$, H^+, Li^+, Na^+, K^+, Ni^{2+}, Co^{2+}, Cu^{2+}) in 1 mL of 1×10^{-2} M PC_n/C_6H_6 solution overnight. The solvent was removed by flowing nitrogen over the sample for about 2 h. Thus all the samples contain the same amount of PC_n. For EPR measurements the same amount (0.3 g) of PC_n (n = 1, 3, 6, 10) impregnated dried Clino powder was transferred into Suprasil quartz tubes (2 mm i.d. × 3 mm o.d.) which were sealed at one end. The filled sample tubes were then flame sealed at the other end. For diffuse reflectance experiments the samples were loaded into a cylindrical quartz sample cell (22 mm diameter × 2 cm path length). All the samples were prepared in the dark to minimize exposure to visible light.

Results

The synthetic Na,K-clinoptilolite zeolites after ion-exchange with H^+, Li^+, Na^+, K^+, Ni^{2+}, Co^{2+} or Cu^{2+} have similar X-ray diffraction patterns to Na,K-clinoptilolite zeolite.[26] This verifies that the Na,K-clinoptilolite structure was retained after ion-exchange with different metal ions and calcination.

Hydrated Na,K-Clino impregnated with PC_n was colorless and EPR silent before and after photoirradiation at room temperature. However, samples of dehydrated M-clinoptilolite

($M = Na^+ + K^+$, H^+, Li^+, Na^+, K^+, Ni^{2+}, Co^{2+} or Cu^{2+}) impregnated with PC_n molecules are light pink, except for Cu^{2+} which is darker pink, and show very weak EPR signals of $PC_n^{\cdot+}$ at $g = 2.006$ with partially resolved hyperfine splitting[21] before irradiation as shown in Fig. 2. This shows that some $PC_n^{\cdot+}$ radical cations are produced during sample preparation in a "dark" reaction. Cu-Clino shows the largest "dark" reaction. After being irradiated by 320 nm light at room temperature for 60 min, the samples turn deep pink and show strong EPR signals (Fig. 2) at $g = 2.006$. This EPR signal and the deep pink color are typical of PC_n^+ radical cations.[21] The EPR signal intensity of M-clinoptilolite/PC_n reaches a plateau after 60 min photoirradiation at room temperature. The spectral widths of the EPR spectra are consistent with those of PC_n^+ in layered materials,[13] silica gel,[16] microporous[21,22] and mesoporous[23] materials. This indicates photoinduced formation of PC_n^+ at room temperature in M-clinoptilolite ($M = Na^+ + K^+$, H^+, Li^+, Na^+, K^+, Ni^{2+}, Co^{2+}, Cu^{2+}). The partially resolved EPR spectra of PC_n^+ radical cations at room temperature show that the radicals have some mobility in the channels of M-clinoptilolite samples at room temperature. The deep pink color of the samples after photoirradiation is stable when the sample tubes are exposed to air or oxygen for several days. The photoproduced PC_n^+ radical cations in M-clinoptilolite are thus stable to oxygen at room temperature.

Fig. 3 shows EPR signal intensity changes of $PC_1^{\cdot+}$ with irradiation time in M-clinoptilolite ($M = Na^+ + K^+$, H^+, Li^+, Na^+, K^+, Ni^{2+}, Co^{2+}, Cu^{2+}). From Fig. 3 it is seen that the highest photoyield is obtained for H-clinoptilolite/PC_1 followed by Ni-clinoptilolite/PC_1. The EPR signals rapidly increase during the first 20 min of irradiation and then reach a plateau after about 30 min. An irradiation time of 60 min was selected for comparative photoyield and stability studies. The photoyield of H-clinoptilolite/PC_1 is about twofold higher than the photoyield of Na,K-clinoptilolite/PC_1. The changes in EPR signal intensities of transition metal ions in M-clinoptilolite/PC_1 are different from those observed for alkali metal ions in M-clinoptilolite/PC_1 for the same irradiation times. As one can see from Fig. 3, Ni-clinoptilolite/PC_1 enhances the photoyield of $PC_1^{\cdot+}$ radical cations and exhibits maximum photoactivity compared with the other transition metal ions and alkali metal ions used. The presence of different types of cocations in M-clinoptilolite along with PC_1 have a significant influence on the efficiency of photoinduced charge separation.

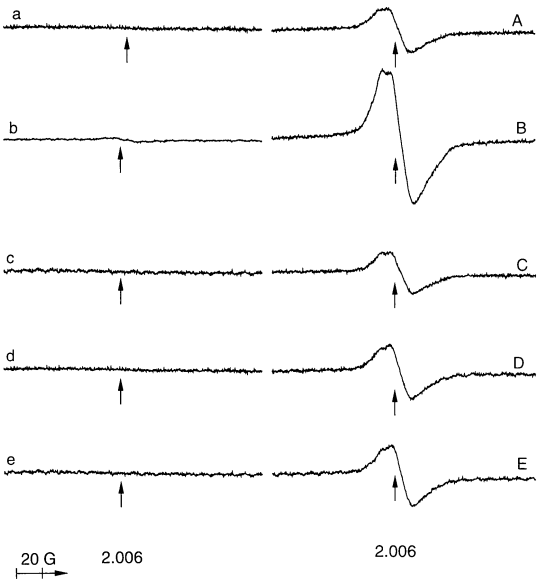

Fig. 2 EPR spectra of Na,K-Clino/PC_1, H-Clino/PC_1, Li Clino/PC_1, Na-Clino/PC_1 and K-Clino/PC_1 samples at room temperature before irradiation (a–e) and after a 60 min room temperature photoirradiation at 320 nm (A–E).

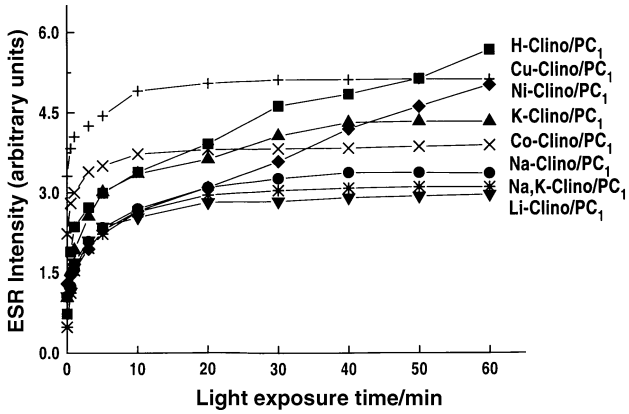

Fig. 3 Room temperature photoinduced $PC_1^{\cdot+}$ radical cation yield measured by EPR *vs.* light exposure time for M-clinoptilolite ($M = Na^+$ K^+, H^+, Li^+, Na^+, K^+, Ni^{2+}, Co^{2+}, Cu^{2+}) samples.

The chain length of PC_n plays a significant role in the photoyield and the stability of the photoinduced PC_n^+ radical cations.[13,23] To examine the effect of alkyl chain length, the photoionization of PC_n was examined for H-clinoptilolite since PC_n impregnated H-clinoptilolite exhibits the maximum activity and stability. The results obtained from photoionization of H-clinoptilolite/PC_n ($n = 1$, 3, 6, 10) are shown in Fig. 4. It can be seen that the PC_n^+ photoyields decrease with increasing alkyl chain length from methylphenothiazine (PC_1) to decylphenothiazine (PC_{10}). There is also a significant increase in the stability of PC_n^+ in M-clinoptilolite/PC_n from PC_1 to PC_{10}. It is clear that the photooxidation yield of PC_n to PC_n^+ depends strongly on the alkyl chain length. The H-clinoptilolite/PC_n changes from light pink to green as the alkyl chain length increases beyond PC_6.

Figs. 5 and 6 show diffuse reflectance spectra of PC_1 in Na,K-Clino and PC_{10} in H-Clino before irradiation and after different irradiation times at room temperature. These spectra are the same as the spectra of PC_n^+ in microporous[21,22] and mesoporous[23] materials in the region from 300 to 800 nm. A prominent band around 515 nm is seen. This supports the existence of PC_n^+ in photoirradiated M-clinoptilolite and further confirms the photooxidation of PC_n into PC_n^+ in M-clinoptilolite.

Fig. 7 shows the structure of the *N*-alkylphenothiazines. The diameters of PC_1, PC_3, PC_6 and PC_{10} are about 6.5, 8, 11 and 14 Å, respectively. Since M-clinoptilolite is a channel type zeolite with a main 10-ring channel with an elliptical

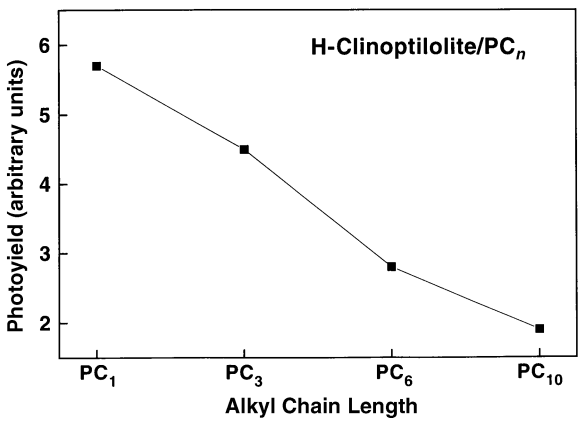

Fig. 4 Room temperature photoyield of H-clinoptilolite/PC_n, where $n = 1$, 3, 6, 10, measured by EPR after 60 min photoirradiation at room temperature *vs.* the pendent alkyl chain length of the *N*-alkylphenothiazine.

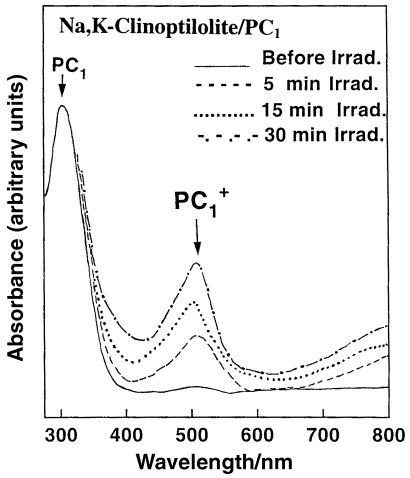

Fig. 5 UV–vis diffuse reflectance spectra of Na,K-clinoptilolite/PC_1 samples at room temperature before irradiation and after 5, 15 and 30 min room temperature photoirradiations at 320 nm.

channel opening of 7.2 × 4.4 Å, it is unclear how much different PC_n ($n = 1$, 3, 6, 10) molecules penetrate into M-clinoptilolite ($M = Na^+ + K^+$, H^+, Li^+, Na^+, K^+, Ni^{2+}, Co^{2+}, Cu^{2+}). To clarify this situation, Fig. 8 shows TGA results obtained from the incorporation of PC_n ($n = 1$, 3, 10) molecules into H-clinoptilolite. All three curves typically show three weight losses, the first near 100 °C assigned to water desorption, the second near 200 °C assigned to *N*-alkylphenothiazine desorption, and the third broad peak centered around 470 °C which is assigned to decomposition of

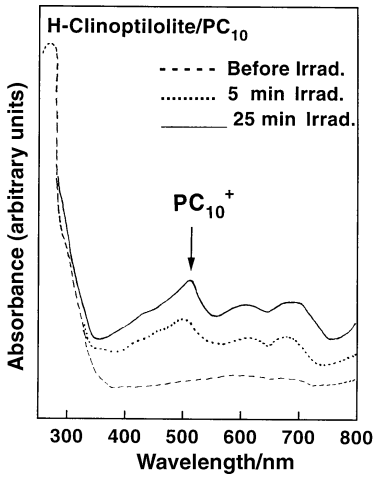

Fig. 6 UV–vis diffuse reflectance spectra of H-clinoptilolite/PC_{10} samples at room temperature before irradiation and after 5 and 25 min room temperature photoirradiations at 320 nm.

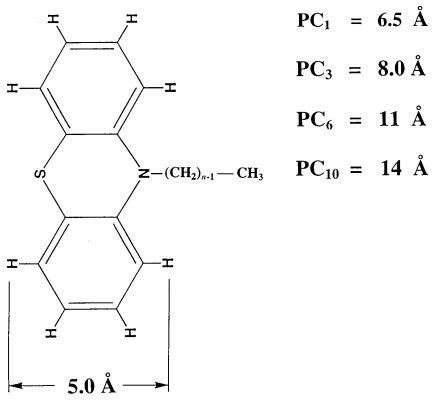

Fig. 7 Structure of *N*-alkylphenothiazines.

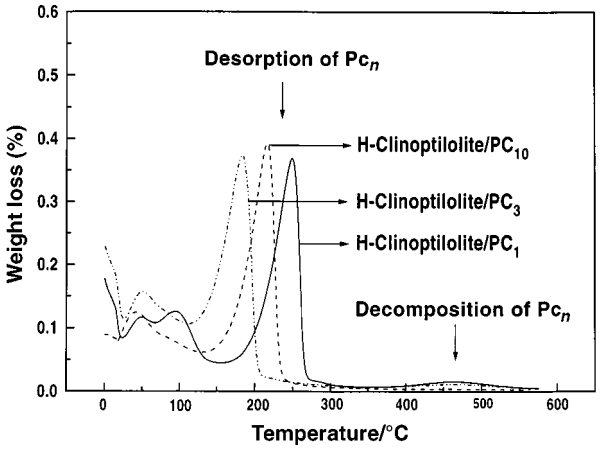

Fig. 8 Differential thermal analysis of H-clinoptilolite/PC_n ($n = 1$, 3, 10).

N-alkylphenothiazine in an oxygen atmosphere. This 470 °C peak is not observed when the experiments are performed under a nitrogen atmosphere. From the TGA results (Fig. 8), we conclude that PC_1 penetrates to a large extent into H-clinoptilolite channels and that PC_n only partially penetrates as the alkyl chain length increases, depending on the estimated molecular diameter. This is consistent with the photoionization results for H-clinoptilolite/PC_n ($n = 1$, 3, 6, 10) which show a decreasing photoyield in the order H-clinoptilolite/PC_1 > H-clinoptilolite/PC_3 > H-clinoptilolite/PC_6 > H-clinoptilolite/PC_{10}.

Discussion

Electron paramagnetic spin resonance and diffuse reflectance results can be used to confirm the existence and identification of radical species. In the present study EPR and diffuse reflectance were used to detect the radicals present following photoirradiation of PC_n in M-clinoptilolite ($M = Na^+ + K^+$, H^+, Li^+, Na^+, K^+, Ni^{2+}, Co^{2+}, Cu^{2+}). Hydrated Na,K-clinoptilolite/PC_n showed no EPR signal at room temperature or 77 K following photoirradiation at room temperature probably due to blocking of the main channels by water molecules. However, photoirradiated, dehydrated M-clinoptilolite/PC_n materials show EPR signals of $PC_n^{\cdot+}$ radical cations. Fig. 2 shows the EPR signals of PC_1^+ in M-clinoptilolite ($M = Na^+ + K^+$, H^+, Li^+, Na^+, K^+) after 60 min irradiation at room temperature. The *g*-factor (2.006) and the color of irradiated M-clinoptilolite/PC_n clearly indicate that the only species present following photoirradiation is $PC_n^{\cdot+}$ (Fig. 2). The intensity changes of the EPR signal due to PC_1^+ with photoirradiation time for M-clinoptilolite/PC_1 ($M = Na^+ + K^+$, H^+, Li^+, Na^+, K^+, Ni^{2+}, Co^{2+}, Cu^{2+}) in Fig. 3 suggest that protons, alkali metal ions and transition metal ions assist the photoionization of PC_1 in M-clinoptilolite. The role of protons as well as metal ions as electron acceptors is evident since there is net photoionization of PC_1 in H-clinoptilolite and M-clinoptilolite. Note that the dark reaction yield at 0 min photoirradiation varies with the metal ion and must be subtracted to obtain the net photoyield. The net photoionization efficiency decreases in the order H-clinoptilolite/PC_1 > Ni-clinoptilolite/PC_1 > K-clinoptilolite/PC_1 > Na-clinoptilolite/PC_1 > Co-clinoptilolite/PC_1 > Na,K-clinoptilolite/PC_1 > Li-clinoptilolite/PC_1 > Cu-clinoptilolite/PC_1. Thus the photoionization efficiency is controlled by the nature of the metal ion in the ion-exchange sites of M-clinoptilolite.

In other photoionization systems,[20,27–29] protons and alkali metal ions have been found to act as electron acceptors. Previous photoionization results from our laboratory[21] demonstrate that long-lived charge separation can be achieved

at room temperature in Na,K-ETS-10 by ion-exchange with protons, alkali metal ions and transition metal ions.

The photoyield trend with alkyl chain length shown in Fig. 4 indicates that the photooxidation yield decreases with an increase in alkyl chain length from PC_1 to PC_3 to PC_6 to PC_{10} in H-clinoptilolite/PC_n and similar behavior is observed in M-clinoptilolite/PC_n. The decrease in photoyield observed from PC_1 to PC_{10} is most probably a result of the restricted diffusion for larger molecules in the channels of M-clinoptilolite.

The decrease in photoyield of PC_n^+ with alkyl chain length is suggested to be due to an increasing propensity to generate aggregates with increasing chain length.[30,31] The formation of such aggregates will lower the rate of diffusion of PC_n into M-clinoptilolite and lead to a diminished photoyield. Diffuse reflectance of H-clinoptilolite/PC_{10} (Fig. 6) also suggests the formation of aggregates by the additional absorption between 600 to 750 nm as the alkyl chain length increases from PC_1 to PC_{10} (compare Fig. 5 and 6). The green color of photoirradiated M-clinoptilolite/PC_n at longer alkyl chain lengths also supports this. Earlier, several workers have observed the formation of a green solution in oxidation reactions of PC_n molecules[30,31] and suggested the formation of molecular aggregates.

The channel diameter of M-clinoptilolite is 7.2 Å which can only accommodate a molecule of $\leqslant$7.2 Å. The main channel opening of M-clinoptilolite is larger than the size of PC_1, so molecules such as PC_1 can completely penetrate into M-clinoptilolites. However, molecules such as PC_3, PC_6 or PC_{10} have larger diameters so these molecules are adsorbed more on the external surface of M-clinoptilolites and only partly penetrate into the channels. Fig. 8 shows TGA results for H-clinoptilolite/PC_n. The TGA results suggest that PC_1 penetrates to a significant extent and that other PC_n molecules only partially penetrate into the channels of H-clinoptilolite. This is consistent with the photoionization results which show a decreased yield with longer alkyl chain length (Fig. 4). The stability of PC_n^+ increases from PC_1 to PC_{10} due to an increased inductive effect in PC_n^+ as a function of longer alkyl chains.[13,21,32] The stability of PC_n^+ in M-clinoptilolites ranges from a few days to several weeks at room temperature depending on the specific metal ion which may be related to its electron affinity within clinoptilolite. It is noteworthy that the photoyield efficiency for PC_1 in H-Clino and Ni-Clino is about twice that of PC_1 in the vanadium silicoaluminophosphate VAPO-5.[33]

Conclusions

Long-lived charge separated states can be formed photochemically in synthetic M-clinoptilolite/PC_n (M = $Na^+ + K^+$, H^+, Li^+, Na^+, K^+, Ni^{2+}, Co^{2+}, Cu^{2+}; n = 1, 3, 6, 10) molecular sieves at room temperature. The PC_n^+ radical cation photoyield depends on the nature of the metal ion in the ion-exchange sites of M-clinoptilolite samples. H-clinoptilolite/PC_n has the highest photoyield followed by Ni-clinoptilolite/PC_n when compared to other M-clinoptilolite/PC_n materials. The PC_n^+ photoyield and stability are also dependent on the alkyl chain length. The PC_n^+ photoyield decreases in the order H-clinoptilolite > Ni-clinoptilolite > K-clinoptilolite > Na-clinoptilolite > Co-clinoptilolite > Na, K-clinoptilolite > Li-clinoptilolite > Cu-clinoptilolite. These results demonstrate some of the size/shape selectivity features of synthetic M-clinoptilolite molecular sieves on such photochemical reactions. The results also suggest that achievement of stable photooxidation at room temperature may make it possible to use these materials for efficient conversion and storage of photochemical energy.

Acknowledgement

This research was supported by the Chemical Sciences, Geosciences and Biosciences Division, Office of Basic Energy Sciences, Office of Science, U.S. Department of Energy, the Texas Advanced Research Program and the Environmental Institute of Houston.

References

1 M. Gratzel, *Energy Resources through Photochemistry and Catalysis*, Academic Press, New York, 1983.
2 G. J. Meyer, in *Molecular Level Artificial Photosynthetic Materials: Progress in Inorganic Chemistry*, ed. K. D. Karlin, Wiley, New York, 1997, vol. 4, p. 143, 167, 209.
3 K. Kalyanasundaram, *Coord. Chem. Rev.*, 1982, **46**, 159.
4 T. J. Meyer, *Acc. Chem. Res.*, 1989, **22**, 163.
5 M. R. Wasielewski, *Chem. Rev.*, 1992, **92**, 435.
6 A. D. Kirk, *Chem. Rev.*, 1999, **99**, 1607.
7 M. Sakaguchi, P. Baglioni and L. Kevan, *J. Phys. Chem.*, 1992, **96**, 2772.
8 Y. S. Kang, H. J. D. McManus and L. Kevan, *J. Phys. Chem.*, 1993, **97**, 2027.
9 T. M. Miyashita and M. Matsuda, *J. Phys. Chem.*, 1983, **87**, 4527.
10 C. Stenland and L. Kevan, *Radiat. Phys. Chem.*, 1991, **37**, 423.
11 J. R. White and A. J. Bard, *J. Electroanal. Chem.*, 1986, **197**, 233.
12 L. Kovar, R. DellaGuardia and J. K. Thomas, *J. Phys. Chem.*, 1984, **88**, 3595.
13 R. M. Krishna, V. Kurshev and L. Kevan, *Phys. Chem. Chem. Phys.*, 1999, **1**, 2833.
14 L. A. Vermeulen and M. E. Thompson, *Nature*, 1992, **358**, 656.
15 R. M. Krishna and L. Kevan, *Microporous Mesoporous Mater.*, 1999, **32**, 169.
16 B. Xiang and L. Kevan, *Langmuir*, 1994, **10**, 2688.
17 B. Xiang and L. Kevan, *Langmuir*, 1995, **11**, 860.
18 X. Liu, K. K. Liu and J. K. Thomas, *J. Phys. Chem.*, 1989, **93**, 4120.
19 S. Sankaraman, K. B. Yoon, T. Yake and J. Kochi, *J. Am. Chem. Soc.*, 1991, **113**, 1419.
20 P. K. Dutta and W. Turbeville, *J. Phys. Chem.*, 1992, **96**, 9410.
21 R. M. Krishna, A. M. Prakash, V. Kurshev and L. Kevan, *Phys. Chem. Chem. Phys.*, 1999, **1**, 4119.
22 V. Kurshev, A. M. Prakash, R. M. Krishna and L. Kevan, *Microporous Mesoporous Mater.*, 2000, **34**, 9.
23 R. M. Krishna, A. M. Prakash and L. Kevan, *J. Phys. Chem. B*, 2000, **104**, 1796.
24 G. Gottardi and E. Galli, *Natural Zeolites*, Springer-Verlag, Berlin, 1985, p. 256.
25 H. C. Woo, K. H. Lee and J. S. Lee, *Appl. Catal. A*, 1996, **134**, 147.
26 D. Zhao, R. Szostak and L. Kevan, *Energy Lab. Newsl.*, 1997, **34**, 5.
27 (*a*) M. Borja and P. K. Dutta, *Nature*, 1993, **362**, 43; (*b*) M. Ledney and P. K. Dutta, *J. Am. Chem. Soc.*, 1995, **117**, 7687.
28 G. Centi, C. Golinelli and F. Trifiro, *Appl. Catal.*, 1988, **48**, 13.
29 T. Shida, T. Tanaka, T. Funabiki and S. Yoshida, *J. Chem. Soc., Faraday Trans.*, 1998, **94**, 695.
30 R. Foster and R. Hanson, *Biochim. Biophys. Acta*, 1966, **112**, 482.
31 J. Cavanaugh, *J. Am. Chem. Soc.*, 1959, **81**, 2507.
32 L. S. Levitt and H. F. Widing, in *Progress in Physical Organic Chemistry*, ed. R. W. Taft, Wiley, New York, 1976, vol. 12, ch. 5.
33 Z. Chang, R. Koodali, R. M.Krishna, L. Kevan, *J. Phys. Chem. B*, in press